Weierstraß-Institut

für Angewandte Analysis und Stochastik

im Forschungsverbund Berlin e. V.

Preprint ISSN 0946 – 8633

Improving mass conservation in FE approximations of the Navier Stokes equations using continuous velocity fields: A connection between grad-div stabilization and Scott-Vogelius elements

M. A. Case[1], V. J. Ervin[2], A. Linke[3], L. G. Rebholz[4]

submitted: 10 May 2010

[1] Clemson University
email: mcase@clemson.edu

[2] Clemson University
email: vjervin@clemson.edu

[3] Weierstrass Institute for Applied Analysis and Stochastics
email: linke@wias-berlin.de

[4] Clemson University
email: rebholz@clemson.edu

No. 1510
Berlin 2010

2010 *Mathematics Subject Classification.* 76D05 65M60.

Key words and phrases. incompressible Navier-Stokes equations, mixed finite elements, stabilized finite elements, grad-div stabilization, Taylor-Hood element, Scott-Vogelius element.

M. Case, L. Rebholz partially supported by National Science Foundation grant DMS0914478.
V. Ervin partially supported by the US Army Research Office under grant W911NF-05-1-0380.

Edited by
Weierstraß-Institut für Angewandte Analysis und Stochastik (WIAS)
Mohrenstraße 39
10117 Berlin
Germany

Fax: +49 30 2044975
E-Mail: preprint@wias-berlin.de
World Wide Web: http://www.wias-berlin.de/

Abstract

This article studies two methods for obtaining excellent mass conservation in finite element computations of the Navier-Stokes equations using continuous velocity fields. Under mild restrictions, the Scott-Vogelius element pair has recently been shown to be inf-sup stable and have optimal approximation properties, while also providing pointwise mass conservation. We present herein the first numerical tests of this element pair for the time dependent Navier-Stokes equations. We also prove that, again under these mild restrictions, the limit of the grad-div stabilized Taylor-Hood solutions to the Navier-Stokes problem converges to the Scott-Vogelius solution as the stabilization parameter tends to infinity. That is, in this setting, we provide theoretical justification that choosing the parameter large does not destroy the solution. A limiting result is also proven for the general case. Numerical tests are provided which verify the theory, and show how both Scott-Vogelius and grad-div stabilized Taylor-Hood (with large stabilization parameter) elements can provide accurate results with excellent mass conservation for Navier-Stokes approximations.

1 Introduction

This article studies two finite element methods for approximating solutions to the Navier-Stokes equations (NSE) that use continuous velocity fields and provide accurate approximations as well as excellent mass conservation. Under the restriction that the mesh be created as a barycenter refinement of a triangular/tetrahedral mesh, and that the degree k of approximating polynomial for velocity be chosen at least as large as the dimension of the problem, $k \geq d$, the $((P_k)^d, P_{k-1}^{disc})$ pair (called the Scott-Vogelius (SV) pair), has recently been shown to be inf-sup stable and admit optimal approximation properties [34, 33]. Moreover, it has the fundamental physical property that, since $\nabla \cdot (P_k)^d \subset P_{k-1}^{disc}$, the weak enforcement of mass conservation imposed by the usual Galerkin finite element method for Stokes or the NSE actually enforces strong (pointwise) conservation of mass.

The second method studied herein is the Galerkin method for the NSE with Taylor-Hood (TH) elements and grad-div stabilization (with parameter γ). This method is well studied in the general case [24, 26, 6, 16], and it is well known that the stabilization improves mass conservation and relaxes the effect of the pressure error on the velocity error. We show that on a barycenter refined mesh the TH solutions corresponding to a sequence of grad-div parameters $\gamma_n \to \infty$ converge to the SV solution. This provides theoretical justification that one can choose γ significantly larger than $O(1)$ (see [6, 22]), and still obtain an accurate solution with excellent mass conservation, although computationally

care for numerical roundoff error still must be taken. We also prove that on a regular mesh, as $\gamma_n \to \infty$ the TH solutions converge to a solution which is also pointwise mass conservative.

Although the incompressible NSE are one of the most investigated mathematical equations [30, 31, 15, 9, 12, 7, 10, 2, 8, 28, 4], their numerical solution remains a difficult challenge, and new methods and strategies for their solution are regularly proposed. Nevertheless, even in the case of laminar, single phase Newtonian fluids, some important aspects of their numerical approximation are sometimes overlooked, such as the importance of mass conservation [26, 5, 20, 6, 22, 18, 19]. It is well-known that mixed finite element discretizations of the incompressible NSE are prone to different kinds of numerical instabilities, when one combines a certain discrete velocity space X_h in a naive way with a discrete pressure space Q_h. The violation of discrete inf-sup stability [2, 7, 28] is the classical example for when the discrete pressure space is too large in relation to the discrete velocity space. The opposite extreme is when the discrete pressure space is too small. In this case the approximation does not adequately satisfy the conservation of mass equation, thereby giving a poor approximation to the physical solution. It is this second problem that is the motivation of this work.

There are a number of strategies for avoiding poor mass conservation: several element choices are known to provide pointwise mass conservation [34, 33], discontinuous Galerkin methods typically admit local mass conservation [27] (several in fact deliver pointwise divergence-free solutions [3]), penalization techniques such as grad-div stabilization discussed herein reduce global mass conservation error, and a posteriori methods can be used to enforce the conservation of mass on already computed solutions [21]. For each technique, there are naturally both good features and drawbacks, and therefore a determination of which method is "best" is certainly problem dependent.

Still, in most cases, the use of TH elements with grad-div stabilization is one of the easiest to implement. For many years TH elements have been a popular choice of approximating element in fluid flow simulations, and most downloadable finite element packages have some TH elements implemented. Hence getting a TH code and adding grad-div stabilization is typically convenient and simple. However, until now, it was believed that the improvement in mass conservation using grad-div stabilization, although sometimes significant over usual TH solutions, was limited to an $O(1)$ choice of the stabilization parameter. With this limitation, one had to decide whether the provided mass conservation was good enough, or instead if a different element choice or DG should be used. Hence this work provides a simple solution to correct for poor mass conservation in existing codes, and therefore may lead to TH elements being a good choice on a much wider set of problems.

This paper is arranged as follows. In Section 2 we give notation and preliminaries, including a brief discussion of the SV element. In Section 3 we prove that on barycenter refined meshes and $k \geq d$, grad-div stabilized TH solutions of the NSE converge to SV solutions as the grad-div parameter tends to ∞. Discussed in Section 4 is the convergence of the TH approximations as $\gamma_n \to \infty$ on regular meshes. Section 5 presents numerical experiments that illustrate the theory.

2 Preliminaries

We will represent the L^2 norm and inner product by $\|\cdot\|$ and $(\cdot,\cdot)$, respectively. All other norms used will be clearly denoted with subscripts.

Recall the time dependent incompressible NSE on a polygonal (2d), or polyhedral (3d), domain Ω, and for simplicity with homogeneous Dirichlet boundary conditions:

$$\begin{aligned} \mathbf{u}_t - \nu\nabla\mathbf{u} + \mathbf{u}\cdot\nabla\mathbf{u} + \nabla p &= \mathbf{f}, \text{ in } \Omega\times(0,T], && (2.1)\\ \nabla\cdot\mathbf{u} &= 0, \text{ in } \Omega\times(0,T], && (2.2)\\ \mathbf{u}(\mathbf{x},0) &= \mathbf{u}_0, \text{ in } \Omega && (2.3)\\ \mathbf{u} &= \mathbf{0} \text{ on } \partial\Omega\times(0,T]. && (2.4) \end{aligned}$$

Here, $\mathbf{u}$ represents velocity, p the (zero-mean) pressure, $\mathbf{f}$ an external force, and ν the kinematic viscosity.

Throughout the report, $(X_h,Q_h)\subset(H_0^1(\Omega),L_0^2(\Omega))$ will denote either the Taylor-Hood or Scott-Vogelius element pair. For Taylor-Hood elements (X_h,Q_h) are well known to be inf-sup stable. For Scott-Vogelius elements with degree $k\geq d$ and the mesh be constructed by a barycenter refinement of a quasi-uniform mesh (details in the following section), (X_h,Q_h) is inf-sup stable.

The following lemma is used in the analysis below.

Lemma 2.1. *There exists a constant $C^*(\Omega)$, dependent only on the size of Ω, that satisfies $\forall\mathbf{u},\mathbf{v},\mathbf{w}\in H_0^1(\Omega)$,*

$$\begin{aligned} |(\mathbf{u}\cdot\nabla\mathbf{v},\mathbf{w})|+|((\nabla\cdot\mathbf{u})\mathbf{v},\mathbf{w})| &\leq C^*\|\nabla\mathbf{u}\|\,\|\nabla\mathbf{v}\|\,\|\nabla\mathbf{w}\|^{1/2}\|\mathbf{w}\|^{1/2} && (2.5)\\ |(\mathbf{u}\cdot\nabla\mathbf{v},\mathbf{w})|+|((\nabla\cdot\mathbf{u})\mathbf{v},\mathbf{w})| &\leq C^*\|\nabla\mathbf{u}\|\,\|\nabla\mathbf{v}\|\,\|\nabla\mathbf{w}\| && (2.6) \end{aligned}$$

Proof. The first inequality follows from Holder's inequality, Ladyzhenskaya inequalities and the Sobolev imbedding theorem. The second follows directly from the first with the Poincare inequality in $H_0^1(\Omega)$. □

2.1 Scott-Vogelius and Taylor-Hood elements

The SV element pair is not yet very well known, and so we now give a brief description of it. In essence, the SV pair is the same as the TH pair except that
(i) $k\geq d$, where d is the space dimension,
(ii) the pressure space is discontinuous, and
(iii) the mesh is required to be a barycenter refinement of a regular mesh.
That is, polynomials of degree k and $k-1$ are used to approximate the velocity and pressure spaces respectively, with $k\geq d$ (which is only a restriction in 3d compared to TH), and the mesh $\mathcal{T}_h$ that is used must be derived from a regular triangularization (tetrahedralization) of Ω, where each element is refined by connecting its barycenter to the vertices. An illustration of such a refinement is given in Figure 1. With such a mesh

construction and $k \geq d$, it was proved by Zhang in [33] that the SV elements are LBB stable under these restrictions. It is well known that the TH pair is LBB stable for this case [7].

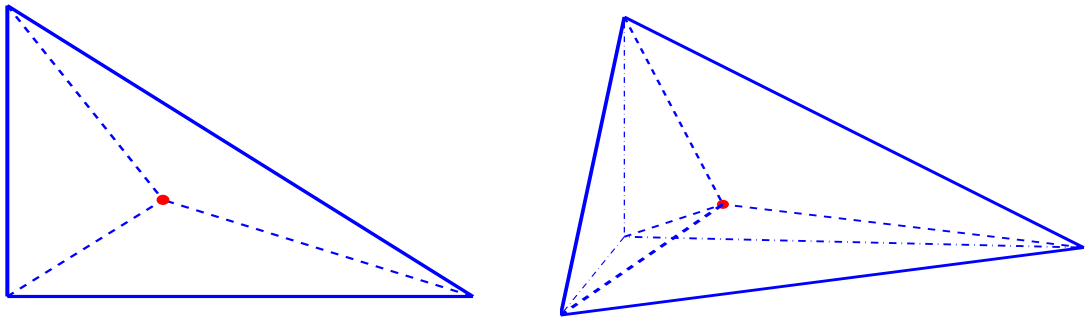

Figure 1: (LEFT) 2d and (RIGHT) 3d macro-element, shown with dashed lines representing barycenter refinements

We now formally define the element pairs. In space dimension d, for both TH and SV elements we define X_h to be the space of continuous element-wise vector functions of polynomial order $k \geq d$ on $\mathscr{T}_h$

$$X_h := \left\{ \mathbf{v}_h \in [C(\Omega)]^d : \mathbf{v}_{h|T} \in [P_k(T)]^d, \text{ for all } T \in \mathscr{T}_h \, , \mathbf{v}_h = \mathbf{0} \text{ on } \partial\Omega \right\}.$$

For Taylor-Hood, we define

$$Q_h^{\mathrm{TH}} := \left\{ q_h \in L^2(\Omega) \cap C(\Omega) : q_{h|T} \in P_{k-1}, \text{ for all } T \in \mathscr{T}_h, \int_\Omega q_h d\Omega = 0 \right\},$$

while the pressure space of the Scott-Vogelius element is only different from Taylor-Hood's in that its pressures are discontinuous:

$$Q_h^{\mathrm{SV}} := \left\{ q_h \in L^2(\Omega) : q_{h|T} \in P_{k-1}, \text{for all } T \in \mathscr{T}_h, \int_\Omega q_h d\Omega = 0 \right\}.$$

Note that the dimension of the pressure space for SV elements is significantly larger than that for TH elements. This creates a greater total number of degrees of freedom needed for linear solves using SV elements, however it is not immediately clear whether this will lead to a significant increase in computational time if preconditioners such as Augmented Lagrangian type are used [1]. The authors plan to consider this questions in future studies.

Although the velocity spaces of the TH and SV elements are the same, the spaces of discretely divergence free subspaces are different, and will be denoted by

$$\begin{aligned} V_h^{SV} &:= \{ \mathbf{v}_h \in X_h \, : (\nabla \cdot \mathbf{v}_h, q_h) = 0, \, \forall q_h \in Q_h^{SV} \} \\ V_h^{TH} &:= \{ \mathbf{v}_h \in X_h \, : (\nabla \cdot \mathbf{v}_h, q_h) = 0, \, \forall q_h \in Q_h^{TH} \}. \end{aligned}$$

The SV element is very interesting from the mass conservation point of view since its discrete velocity space and its discrete pressure space fulfill an important property, namely

$$\nabla \cdot X_h \subset Q_h^{\mathrm{SV}}. \tag{2.7}$$

Thus, using SV elements, weak mass conservation via

$$(\nabla \cdot \mathbf{u}_h, q_h) = 0, \ \forall q_h \in Q_h$$

implies strong (pointwise) mass conservation since we can choose the special test function $q_h = \nabla \cdot \mathbf{u}_h$ to get

$$\|\nabla \cdot \mathbf{u}_h\|^2 = 0.$$

In general, the same pressure test function cannot be used in the Taylor-Hood case, since $\nabla \cdot X_h \not\subset Q_h^{\mathrm{TH}}$. Hence the Taylor-Hood element only delivers discretely divergence-free approximations $\mathbf{u}_h$.

The temporal-spatial discretization we study, for either TH or SV, is the Crank-Nicolson Galerkin method, given in skew-symmetrized form by:
Find $(\mathbf{u}_h^n, p_h^n) \in X_h \times Q_h$ *with* $Q_h \in \{Q_h^{\mathrm{TH}}, Q_h^{\mathrm{SV}}\}$ *such that* $\forall (\mathbf{v}_h, q_h) \in X_h \times Q_h$ *for* $n = 1, 2, \ldots, M = T/\Delta t$,

$$\begin{aligned} \frac{1}{\Delta t}(\mathbf{u}_h^{n+1} - \mathbf{u}_h^n, \mathbf{v}) - (p_h^{n+\frac{1}{2}}, \nabla \cdot \mathbf{v}_h) + \nu(\nabla \mathbf{u}_h^{n+\frac{1}{2}}, \nabla \mathbf{v}_h) \quad &+ \quad \gamma(\nabla \cdot \mathbf{u}_h^{n+\frac{1}{2}}, \nabla \cdot \mathbf{v}_h) \\ + (\mathbf{u}_h^{n+\frac{1}{2}} \cdot \nabla \mathbf{u}_h^{n+\frac{1}{2}}, \mathbf{v}_h) + \frac{1}{2}((\nabla \cdot \mathbf{u}_h^{n+\frac{1}{2}})\mathbf{u}_h^{n+\frac{1}{2}}, \mathbf{v}_h) \quad &= \quad (\mathbf{f}^{n+\frac{1}{2}}, \mathbf{v}_h) \qquad (2.8) \\ (\nabla \cdot \mathbf{u}_h^{n+1}, q_h) \quad &= \quad 0. \qquad (2.9) \end{aligned}$$

For the discrete initial velocity, $\mathbf{u}_h^0$ we impose zero pointwise divergence for the initial condition for both SV or TH elements: $\forall (\mathbf{v}_h, q_h) \in (X_h, Q_h^{SV})$,

$$(\mathbf{u}_h^0, \mathbf{v}_h) + (\lambda_h, \nabla \cdot \mathbf{v}_h) + (\nabla \cdot \mathbf{u}_h^0, q_h) = (\mathbf{u}_0, \mathbf{v}_h). \tag{2.10}$$

This condition is necessary for TH elements due to the Crank-Nicolson temporal discretization and our enforcement of discrete mass conservation (2.9). For the backward Euler method, this would not be necessary. However, it is easy to implement.

Throughout we assume that the discrete approximating system of equations is uniquely solvable. We refer the interested reader to [15, 31] for discussions on the unique solvability of (2.8)-(2.9).

3 Relationship between the Taylor-Hood and the Scott-Vogelius element

Section 2 shows the Taylor-Hood and the Scott-Vogelius element are not unrelated to each other, as they differ only in their pressure space. But it turns out that much more can be said. For example, it is relatively easy to show that the H^1 projection of the TH

solution to the Stokes problem into the space of divergence free functions is the SV solution of that Stokes problem (independent of grad-div stabilization). However, the results for the NSE are much more interesting.

We prove, under the mild restrictions under which SV elements are LBB stable, that as $\gamma \to \infty$, the TH solutions to (2.8)-(2.10) converge to the SV solution. Roughly speaking, this result can be understood in the following sense: Under the mesh restriction discussed above and with $k \geq d$, the grad-div stabilized TH solutions "live between" the TH and SV solutions, which are both LBB stable and have optimal approximation properties. Thus, raising γ significantly larger than $O(1)$ in TH computations can provide excellent mass conservation without "destroying" the solution.

Theorem 3.1. *For Δt sufficiently small, $k \geq d$, and using a mesh constructed as a barycenter refinement of a regular mesh, any sequence $\{\mathbf{u}_h\}_{\gamma_i}$ of TH velocity solutions to* (2.8)-(2.10) *converges to the SV velocity solution as the grad-div parameter $\gamma_i \to \infty$. The corresponding TH "modified pressure" solutions $\{p_h - \gamma_i \nabla \cdot \mathbf{u}_h\}_{\gamma_i}$ converge to the SV pressure solution.*

Proof. We begin by noting the a priori bound on the SV and TH solutions, which can be found by choosing the test function $\mathbf{v}_h = \mathbf{u}_h^{n+1/2}$ in (2.8): *For* $0 \leq j \leq M$

$$\left\|\mathbf{u}_h^j\right\|^2 + \Delta t \sum_{n=0}^{j-1} \left(\nu \left\|\nabla \mathbf{u}_h^{n+1/2}\right\|^2 + 2\gamma \left\|\nabla \cdot \mathbf{u}_h^{n+1/2}\right\|^2 \right) \leq \frac{\Delta t}{\nu} \sum_{n=0}^{j-1} \left\|\mathbf{f}^{n+1/2}\right\|_*^2 + \left\|u_h^0\right\|^2 = C(data), \quad (3.1)$$

where $\|\cdot\|_*$ denotes the norm in X^*, the dual space of $X = H_0^1(\Omega)$ endowed with the norm $\|\mathbf{v}\|_X := \|\nabla \mathbf{v}\|$. (For the SV solution $\left\|\nabla \cdot \mathbf{u}_h^{n+1/2}\right\| = 0$.)

In addition, by assumption of the existence and uniqueness of the SV solution (which is independent of γ) and LBB stability we have the SV pressure is bounded independent of γ. In particular we have that for $2 \leq j \leq M$

$$\Delta t \sum_{n=0}^{j-1} \left\|p_{SV}^{n+1/2}\right\|^2 \leq C(data). \quad (3.2)$$

Note that from (3.1) it follows that as $\gamma \to \infty$, $\nabla \cdot \mathbf{u}_h^{n+1/2} \to 0$ for $n = 0, \ldots M-1$. Also, as $\nabla \cdot \mathbf{u}_h^0 = 0$, then $\nabla \cdot \mathbf{u}_h^{n+1} \to 0$ for $n = 0, \ldots M-1$. In addition, as $\left\|\mathbf{u}_h^j\right\|^2$ is uniformly bounded, then the terms $\left\|\nabla \mathbf{u}_h^j\right\|^2$ and $\left\|\nabla \cdot \mathbf{u}_h^j\right\|^2$ are also uniformly bounded. In these later cases the bound will depend upon the mesh parameter h. However, as we are discussing convergence on a fixed mesh, this dependence is not important.

Let $\mathbf{e} := \mathbf{u}_{SV} - \mathbf{u}_{TH} \in V_h^{TH}$, where $(\mathbf{u}_{SV}, p_{SV})$ and $(\mathbf{u}_{TH}, p_{TH})$ denote the SV and TH solutions respectively. (For convenience, in this proof we suppress the dependence on h.)

For $\mathbf{v} \in V_h^{TH}$, we have that $(p_{TH}^{n+\frac{1}{2}}, \nabla \cdot \mathbf{v}) = 0$ and thus that

$$\begin{aligned}\frac{1}{\Delta t}(\mathbf{e}^{n+1} - \mathbf{e}^n, \mathbf{v}) - (p_{SV}^{n+\frac{1}{2}}, \nabla \cdot \mathbf{v}) + \nu(\nabla \mathbf{e}^{n+\frac{1}{2}}, \nabla \mathbf{v}) + \gamma(\nabla \cdot \mathbf{e}^{n+\frac{1}{2}}, \nabla \cdot \mathbf{v}) \\ + (\mathbf{u}_{SV}^{n+\frac{1}{2}} \cdot \nabla \mathbf{u}_{SV}^{n+\frac{1}{2}}, \mathbf{v}) - (\mathbf{u}_{TH}^{n+\frac{1}{2}} \cdot \nabla \mathbf{u}_{TH}^{n+\frac{1}{2}}, \mathbf{v}) + \frac{1}{2}((\operatorname{div} \mathbf{u}_{SV}^{n+\frac{1}{2}})\mathbf{u}_{SV}^{n+\frac{1}{2}}, \mathbf{v}) \\ - \frac{1}{2}((\operatorname{div} \mathbf{u}_{TH}^{n+\frac{1}{2}})\mathbf{u}_{TH}^{n+\frac{1}{2}}, \mathbf{v}) = \mathbf{0}, \quad (3.3)\end{aligned}$$

which can be written as

$$\begin{aligned}\frac{1}{\Delta t}(\mathbf{e}^{n+1} - \mathbf{e}^n, \mathbf{v}) + \nu(\nabla \mathbf{e}^{n+\frac{1}{2}}, \nabla \mathbf{v}) + \gamma(\nabla \cdot \mathbf{e}^{n+\frac{1}{2}}, \nabla \cdot \mathbf{v}) \\ = -(\mathbf{e}^{n+1/2} \cdot \nabla \mathbf{u}_{SV}^{n+\frac{1}{2}}, \mathbf{v}) - (\mathbf{u}_{TH}^{n+\frac{1}{2}} \cdot \nabla \mathbf{e}^{n+1/2}, \mathbf{v}) - \frac{1}{2}((\operatorname{div} \mathbf{e}^{n+1/2})\mathbf{u}_{SV}^{n+\frac{1}{2}}, \mathbf{v}) \\ - \frac{1}{2}((\operatorname{div} \mathbf{u}_{TH}^{n+\frac{1}{2}})\mathbf{e}^{n+1/2}, \mathbf{v}) + (p_{SV}^{n+\frac{1}{2}}, \nabla \cdot \mathbf{v}). \quad (3.4)\end{aligned}$$

With $\mathbf{v} = \mathbf{e}^{n+\frac{1}{2}}$, the identity

$$(\mathbf{u}_{TH}^{n+\frac{1}{2}} \cdot \nabla \mathbf{e}^{n+1/2}, \mathbf{e}^{n+\frac{1}{2}}) + \frac{1}{2}((\operatorname{div} \mathbf{u}_{TH}^{n+\frac{1}{2}})\mathbf{e}^{n+1/2}, \mathbf{e}^{n+\frac{1}{2}}) = 0,$$

and using Lemma 2.1, equation (3.4) becomes

$$\begin{aligned}&\frac{1}{2\Delta t}(\|\mathbf{e}^{n+1}\|^2 - \|\mathbf{e}^n\|^2) + \nu \left\|\nabla \mathbf{e}^{n+1/2}\right\|^2 + \gamma \left\|\nabla \cdot \mathbf{e}^{n+1/2}\right\|^2 \\ = \; & -\frac{1}{2}((\operatorname{div} \mathbf{e}^{n+\frac{1}{2}})\mathbf{u}_{SV}^{n+\frac{1}{2}}, \mathbf{e}^{n+1/2}) - (\mathbf{e}^{n+\frac{1}{2}} \cdot \nabla \mathbf{u}_{SV}^{n+\frac{1}{2}}, \mathbf{e}^{n+1/2}) + (p_{SV}^{n+\frac{1}{2}}, \nabla \cdot \mathbf{e}^{n+1/2}) \\ \leq \; & C \left\|\nabla \mathbf{e}^{n+1/2}\right\|^2 \left\|\nabla \mathbf{u}_{SV}^{n+1/2}\right\| + \left\|p_{SV}^{n+\frac{1}{2}}\right\| \left\|\nabla \cdot \mathbf{e}^{n+1/2}\right\|. \quad (3.5)\end{aligned}$$

Since the mesh is fixed, uniform boundedness, finite dimensionality of $\mathbf{u}_{SV}^{n+\frac{1}{2}}$, and Young's inequality imply

$$\begin{aligned}&\frac{1}{2\Delta t}(\|\mathbf{e}^{n+1}\|^2 - \|\mathbf{e}^n\|^2) + \nu \left\|\nabla \mathbf{e}^{n+1/2}\right\|^2 + \gamma \left\|\nabla \cdot \mathbf{e}^{n+1/2}\right\|^2 \\ \leq \; & C \left\|\mathbf{e}^{n+1/2}\right\|^2 + \frac{\gamma}{2} \left\|\nabla \cdot \mathbf{e}^{n+1/2}\right\|^2 + \frac{1}{2\gamma} \left\|p_{SV}^{n+1/2}\right\|^2. \quad (3.6)\end{aligned}$$

With $\|\mathbf{e}^0\| = 0$, subtracting $\frac{\gamma}{2} \left\|\nabla \cdot \mathbf{e}^{n+1/2}\right\|^2$ from both sides of (3.6), then summing from $n = 0$ to $j-1$, $2 \leq j \leq M$, we have

$$\begin{aligned}\|\mathbf{e}^j\|^2 + \Delta t \sum_{n=0}^{j-1} \left(2\nu \left\|\nabla \mathbf{e}^{n+1/2}\right\|^2 + \gamma \left\|\nabla \cdot \mathbf{e}^{n+1/2}\right\|^2\right) \\ \leq C\Delta t \sum_{n=0}^{j} \|\mathbf{e}^n\|^2 + \frac{\Delta t}{\gamma} \sum_{n=0}^{j-1} \left\|p_{SV}^{n+1/2}\right\|^2. \quad (3.7)\end{aligned}$$

The discrete Gronwall inequality [11] then implies that (for Δt sufficiently small)

$$\left\|\mathbf{e}^j\right\|^2 + \Delta t \sum_{n=0}^{j-1}\left(2\nu\left\|\nabla\mathbf{e}^{n+1/2}\right\|^2+\gamma\left\|\nabla\cdot\mathbf{e}^{n+1/2}\right\|^2\right) \leq C\frac{\Delta t}{\gamma}\sum_{n=0}^{j-1}\left\|p_{SV}^{n+1/2}\right\|^2 \leq C\frac{1}{\gamma}.$$

Hence, as $\gamma\to\infty$, $\left\|\mathbf{e}^j\right\|\to 0$, $j=1,2,\ldots,M$, i.e. $\mathbf{u}_{TH}\to\mathbf{u}_{SV}$.

With the convergence of the velocity established, we now prove convergence of the modified TH pressure to the SV pressure. Subtracting the TH solution from the SV solution, and using the notation as above, we get $\forall\mathbf{v}_h\in X_h$,

$$\begin{aligned}&((p_{TH}^{n+\frac{1}{2}}-\gamma\nabla\cdot\mathbf{u}_{TH}^{n+\frac{1}{2}})-p_{SV}^{n+\frac{1}{2}},\nabla\cdot\mathbf{v}_h)=\frac{1}{\Delta t}(\mathbf{e}^{n+1}-\mathbf{e}^n,\mathbf{v}_h)+\nu(\nabla\mathbf{e}^{n+\frac{1}{2}},\nabla\mathbf{v}_h)\\&+(\mathbf{e}^{n+\frac{1}{2}}\cdot\nabla\mathbf{u}_{TH}^{n+\frac{1}{2}},\mathbf{v}_h)+(\mathbf{u}_{SV}^{n+\frac{1}{2}}\cdot\nabla\mathbf{e}^{n+\frac{1}{2}},\mathbf{v}_h)+\frac{1}{2}((\nabla\cdot\mathbf{e}^{n+\frac{1}{2}})\mathbf{u}_{TH}^{n+\frac{1}{2}},\mathbf{v}_h)+\frac{1}{2}((\nabla\cdot\mathbf{u}_{SV}^{n+\frac{1}{2}})\mathbf{e}^{n+\frac{1}{2}},\mathbf{v}_h)\end{aligned} \tag{3.8}$$

Now dividing both sides by $\|\nabla\mathbf{v}_h\|$, applying Lemma 2.1 and Cauchy-Schwarz to the right hand side, again using that solutions are uniformly bounded, then reducing, gives

$$\frac{((p_{TH}^{n+\frac{1}{2}}-\gamma\nabla\cdot\mathbf{u}_{TH}^{n+\frac{1}{2}})-p_{SV}^{n+\frac{1}{2}},\nabla\cdot\mathbf{v}_h)}{\|\nabla\mathbf{v}_h\|}\leq C(\|\mathbf{e}^n\|+\left\|\mathbf{e}^{n+1}\right\|). \tag{3.9}$$

Since $(p_{TH}^{n+\frac{1}{2}}-\gamma\nabla\cdot\mathbf{u}_{TH}^{n+\frac{1}{2}})\in Q_h^{SV}$ and the restriction on the mesh and k are such that SV elements are LBB stable, the inf-sup condition for (X_h,Q_h^{SV}) implies

$$\left\|(p_{TH}^{n+\frac{1}{2}}-\gamma\nabla\cdot\mathbf{u}_{TH}^{n+\frac{1}{2}})-p_{SV}^{n+\frac{1}{2}}\right\|\leq C(\|\mathbf{e}^n\|+\left\|\mathbf{e}^{n+1}\right\|), \tag{3.10}$$

and thus since $\mathbf{e}\to\mathbf{0}$, we have that

$$\left\|(p_{TH}^{n+\frac{1}{2}}-\gamma\nabla\cdot\mathbf{u}_{TH}^{n+\frac{1}{2}})-p_{SV}^{n+\frac{1}{2}}\right\|\to 0. \tag{3.11}$$

Note that since it is the time-level $n+\frac{1}{2}$ pressures that are directly solved for in the Crank-Nicolson scheme, it is this convergence result that is relevant, not the n or $n+1$ time levels. □

3.1 A connection for the steady NSE problem

An analogous result as proved above holds for the steady NSE. Consider the usual skew symmetrized finite element scheme for the NSE [15]: *Find* $(\mathbf{u}_h,p_h)\in(X_h,Q_h)$ *satisfying* $\forall(\mathbf{v}_h,q_h)\in(X_h,Q_h)$

$$\begin{aligned}\nu(\nabla\mathbf{u}_h,\nabla\mathbf{v}_h)-(p_h,\nabla\cdot\mathbf{v}_h)+\gamma(\nabla\cdot\mathbf{u}_h,\nabla\cdot\mathbf{v}_h)+(\mathbf{u}_h\cdot\nabla\mathbf{u}_h,\mathbf{v}_h)&\\+\frac{1}{2}((\mathrm{div}\,\mathbf{u}_h)\mathbf{u}_h,\mathbf{v}_h)&=(\mathbf{f},\mathbf{v}_h), \quad (3.12)\\(\nabla\cdot\mathbf{u}_h,q_h)&=0, \quad (3.13)\end{aligned}$$

where Q_h is either Q_h^{SV} or Q_h^{TH}. Note if $Q_h = Q_h^{SV}$, then trivially $\frac{1}{2}((\mathrm{div}\,\mathbf{u}_h)\mathbf{u}_h, \mathbf{v}_h) = \gamma(\nabla \cdot \mathbf{u}_h, \nabla \cdot \mathbf{v}_h) = 0$.

Theorem 3.2. *If the mesh is created as a barycenter refinement of a regular mesh and $k \geq d$, then any sequence $\{\mathbf{u}_h\}_{\gamma_i}$ of TH velocity solutions to* (3.12)-(3.13) *converges to the SV velocity solution as the grad-div parameter $\gamma_i \to \infty$. The corresponding sequence of TH "modified pressure" solutions, $\{p_h - \gamma_i \nabla \cdot \mathbf{u}_h\}_{\gamma_i}$, converge to the SV pressure.*

Remark 3.1. *In the case of non-unique solution, a similar proof to the one below can be used to show that a subsequence of TH solutions will converge to a SV solution.*

Proof. For notational convenience, in the proof we surpress the dependence on h.

We begin by noting the a priori bound, analogous to (3.1), for the steady state approximations.

$$\nu \|\nabla \mathbf{u}\|^2 + 2\gamma \|\nabla \cdot \mathbf{u}\|^2 \leq \frac{1}{\nu} \|\mathbf{f}\|_*^2 \;=\; C(data)\,, \tag{3.14}$$

where, for the SV approximation, $\|\nabla \cdot \mathbf{u}\| = 0$.

Let $\{\gamma_i\}_{i=1}^{\infty} \to \infty$ and $\mathbf{u}_i$ denote the corresponding TH velocity solutions to (3.12)-(3.13). Then, as $\mathbf{u}_i$ is a bounded sequence in a finite dimensional space, we have that there exists $\mathbf{w} \in X_h$ such that a subsequence $\mathbf{u}_{i'} \to \mathbf{w}$. From (3.12)-(3.13) with $\mathbf{v} = \mathbf{u}_i$, $q = p$, we have that

$$\|\nabla \cdot \mathbf{u}_i\| \;\leq\; \frac{1}{\gamma_i} \left(\|\mathbf{f}\|_* \| \|\nabla \mathbf{u}_i\| + \nu \|\nabla \mathbf{u}_i\|^2 \right) \;\leq\; \frac{1}{\gamma_i} C\,. \tag{3.15}$$

As $\mathbf{u}_{i'} \to \mathbf{w}$, then $\nabla \cdot \mathbf{u}_{i'} \to \nabla \cdot \mathbf{w}$, (using the equivalence of norms in a finite dimensional space), and as $\|\nabla \cdot \mathbf{u}_{i'}\| \to 0$, we have that

$$\|\nabla \cdot \mathbf{w}\| \;=\; 0\,, \quad \text{i.e. } \mathbf{w} \in V_h^{SV}\,.$$

Next we show that $\mathbf{w} = \mathbf{u}_{SV}$. Consider, for $\mathbf{v} \in V_h^{SV}$

$$|res(\mathbf{v})| \;=\; |\nu(\nabla \mathbf{w}, \nabla \mathbf{v}) + (\mathbf{w} \cdot \nabla \mathbf{w}, \mathbf{v}) - (\mathbf{f}, \mathbf{v})|\,. \tag{3.16}$$

With $\mathbf{e}_{i'} := \mathbf{w} - \mathbf{u}_{i'}$, combining (3.12) ($\mathbf{v} \in V_h^{SV}$) with(3.16),

$$\begin{aligned} |res(\mathbf{v})| &= |\nu(\nabla \mathbf{e}_{i'}, \nabla \mathbf{v}) + (\mathbf{w} \cdot \nabla \mathbf{w}, \mathbf{v}) - (\mathbf{u}_{i'} \cdot \nabla \mathbf{u}_{i'}, \mathbf{v}) - \frac{1}{2}(\mathrm{div}\,(\mathbf{u}_{i'})\mathbf{u}_{i'}, \mathbf{v})| \\ &= |\nu(\nabla \mathbf{e}_{i'}, \nabla \mathbf{v}) + (\mathbf{e}_{i'} \cdot \nabla \mathbf{w}, \mathbf{v}) + (\mathbf{u}_{i'} \cdot \nabla \mathbf{e}_{i'}, \mathbf{v}) - \frac{1}{2}(\mathrm{div}\,(\mathbf{e}_{i'})\mathbf{u}_{i'}, \mathbf{v})| \\ &\leq C \|\mathbf{e}_{i'}\| \|\mathbf{v}\|\,. \end{aligned} \tag{3.17}$$

As $\mathbf{e}_{i'} \to \mathbf{0}$ as $\gamma_{i'} \to \infty$, it follows from the existence and uniqueness of the SV solution to (3.12)-(3.13) that $\mathbf{w} = \mathbf{u}_{SV}$. In addition, from the above argument it immediately follows that the limit of any convergent subsequence of $\{\mathbf{u}_i\}$ must be u_{SV}.

We now show that $\{\mathbf{u}_i\} \to \mathbf{u}_{SV}$. If $\{\mathbf{u}_i\} \not\to \mathbf{u}_{SV}$, then there exists an $\varepsilon > 0$ and a subsequence $\{\mathbf{u}_{i'}\}$ with the property $\|\mathbf{u}_i - \mathbf{u}_{SV}\| > \varepsilon$. However, as $\{\mathbf{u}_{i'}\}$ is a bounded sequence in a finite dimensional space, it has a convergent subsequence $\{\mathbf{u}_{i''}\}$. From above we have that $\{\mathbf{u}_{i''}\} \to \mathbf{u}_{SV}$, which contradicts $\|\mathbf{u}_{i'} - \mathbf{u}_{SV}\| > \varepsilon$. Thus $\{\mathbf{u}_i\} \to \mathbf{u}_{SV}$.

With the convergence of the velocity established, the convergence of the TH modified pressure solutions to the SV pressure solution follows analogously to the time-dependent case.

□

4 Convergence of the TH approximations as $\gamma \longrightarrow \infty$ in the general case

In Section 3 we showed that, as the grad-div parameter, γ, goes to infinity the TH velocity approximations converge to the SV velocity approximation. The SV approximation, as described above, requires $k \geq d$ and a barycenter refined mesh. In this section we investigate the question of convergence of the TH approximations as $\gamma \longrightarrow \infty$ on a regular mesh and with $k \geq 2$. It is known that taking γ too large in the general case can have an over-stabilizing effect [22], although it is also known that with larger γ comes improved mass conservation. Our intention is to further investigate this phenomena.

4.1 Limiting result

We first show that the approximations converge, and identify the limit function. Analogous to the previous section, it is again a modified pressure that converges to the limit pressure.

We consider the steady-state problem, and the extension to the time dependent case is straight-forward, following Section 3. With the notation as introduced above, let

$$V_h^0 := \{v_h \in X_h : \nabla \cdot v_h|_T = 0, \text{ for all } T \in \mathcal{T}_h\}.$$

Note that $V_h^0 \subset V_h$, and on a barycenter refined mesh $V_h^0 \subset V_h^{SV}$.

Let $\mathbf{z}_h \in V_h^0$ be defined by

$$\nu(\nabla \mathbf{z}_h, \nabla \mathbf{v}_h) + (\mathbf{z}_h \cdot \nabla \mathbf{z}_h, \mathbf{v}_h) = (\mathbf{f}, \mathbf{v}_h), \quad \forall \mathbf{v}_h \in V_h^0. \tag{4.1}$$

We assume existence and uniqueness of $\mathbf{z}_h$. (See [7, 15] for a discussion of existence and uniqueness.) Let $r_h \in Q_h^{TH}$ be defined by

$$(r_h, \nabla \cdot \mathbf{v}_h) = \nu(\nabla \mathbf{z}_h, \nabla \mathbf{v}_h) + (\mathbf{z}_h \cdot \nabla \mathbf{z}_h, \mathbf{v}_h) - (\mathbf{f}, \mathbf{v}_h), \quad \forall \mathbf{v}_h \in (V_h^{TH})^{\perp}, \tag{4.2}$$

where $(V_h^{TH})^{\perp}$ denotes the orthogonal component of V_h^{TH} in X_h with respect to the innerproduct $\langle \mathbf{v}, \mathbf{w} \rangle = (\nabla \mathbf{v}, \nabla \mathbf{w})$. In addition, for $\{\mathbf{u}_h\}_{\gamma_i} \in X_h$, let $\rho_{h,i} \in Q_h^{TH}$ be defined by

$$(\rho_{h,i}, \nabla \cdot \mathbf{v}_h) := (\nabla \cdot \mathbf{u}_{h,i}, \nabla \cdot \mathbf{v}_h), \quad \forall \mathbf{v}_h \in (V_h^{TH})^{\perp}. \tag{4.3}$$

The existence and uniqueness of r_h and $\rho_{h,i}$ follows from (X_h, Q_h^{TH}) satisfying the LBB condition, and the generalized Lax-Milgram theorem.

Theorem 4.1. *For any sequence* $\{(\mathbf{u}_h, p_h)\}_{\gamma_i}$ *of* TH *solutions to* (3.12)-(3.13) *we have that* $\{(\mathbf{u}_h, (p_h - \gamma_i \rho_h))\}_{\gamma_i}$ *converges to* $(\mathbf{z}_h, r_h)$ *as the grad-div parameter* $\gamma_i \to \infty$.

Remark 4.1. *Similar to the limit case for steady NSE in section 3, if the SV solution is not unique, then one can show a subsequence of TH solutions converges to a SV solution.*

Proof. For notational convenience, in the proof we surpress the dependence on h.

With V_h^{SV} replaced by V_h^0, the proof that $\{\mathbf{u}_i\} \to \mathbf{z}$ follows verbatim the proof of Theorem 3.2.

Using the LBB condition, $X_h = V_h^{TH} \oplus (V_h^{TH})^{\perp}$, and $\mathbf{e}_i = \mathbf{z} - \mathbf{u}_i$

$$\begin{aligned}
\beta \|r - (p_i - \gamma_i \rho_i)\| &\leq \sup_{\mathbf{v} \in X_h} \frac{(r, \nabla \cdot \mathbf{v}) - (p_i, \nabla \cdot \mathbf{v}) + (\gamma_i \rho_i, \nabla \cdot \mathbf{v})}{\|\mathbf{v}\|_X} \\
&= \sup_{\mathbf{v} \in (V_h^{TH})^{\perp}} \frac{(r, \nabla \cdot \mathbf{v}) - (p_i, \nabla \cdot \mathbf{v}) + (\gamma_i \rho_i, \nabla \cdot \mathbf{v})}{\|\nabla \mathbf{v}\|} \\
&= \sup_{\mathbf{v} \in (V_h^{TH})^{\perp}} \frac{\nu(\nabla \mathbf{e}_i, \nabla \mathbf{v}) + (\mathbf{z} \cdot \nabla \mathbf{z}, \mathbf{v}) - (\mathbf{u}_i \cdot \nabla \mathbf{u}_i, \mathbf{v}) - \frac{1}{2}(\mathrm{div}\,(\mathbf{u}_i)\mathbf{u}_i, \mathbf{v})}{\|\nabla \mathbf{v}\|} \\
&\leq \nu \|\nabla \mathbf{e}_i\| + \|\mathbf{e}_i \cdot \nabla \mathbf{z}\| + \|\mathbf{u}_i \cdot \nabla \mathbf{e}_i\| + \frac{1}{2}\|\mathrm{div}\,(\mathbf{e}_i)\mathbf{u}_i\|\,.
\end{aligned}$$

From the boundness of $\mathbf{z}$, $\mathbf{u}_i$, and that $\mathbf{e}_i \to \mathbf{0}$ as $\gamma_i \to \infty$, we have that $(p_i - \gamma_i \rho_i) \to r$.

□

4.2 Quality of the limit solution

We also consider in this section the quality of the limit solution. We give examples of meshes where good results would be expected for the limit solution and where very poor results would occur.

As the grad-div parameter $\gamma_i \to \infty$, the TH velocity approximation $\mathbf{u}_h \in V_h^{TH} \to \mathbf{z} \in V_h^0$. So, in the limit, the TH velocity approximation is pointwise mass conservative. However the momentum equation (3.12) only holds for $\mathbf{v}_h$ in the lower dimensional space V_h^0.

Presented in Tables 1 are $dim(X_h)$ (assuming homogeneous boundary conditions for the velocity), $dim(V_h^{TH})/dim(X_h)\%$, and $dim(V_h^0)/dim(X_h)\%$ for several uniform triangulations of the unit square (pictures of 3×3 case shown in Figure 2). Table 2 contains the same statistics for barycenter refined meshes. The dimensions of the spaces were computed using the `rank` command in MATLAB. For both triangulations $dim(V_h^{TH})/dim(X_h)$ is approximately 87%. The $dim(V_h^0)/dim(X_h)$ is slightly higher ($\approx 30\%$) for the regular triangulations than for the barycenter refined triangulations ($\approx 24\%$). Thus in this case, taking γ large will not destroy the solution, and in fact one could expect a better solution from the general mesh than the barycenter refined one for a comparable number of degrees of freedom.

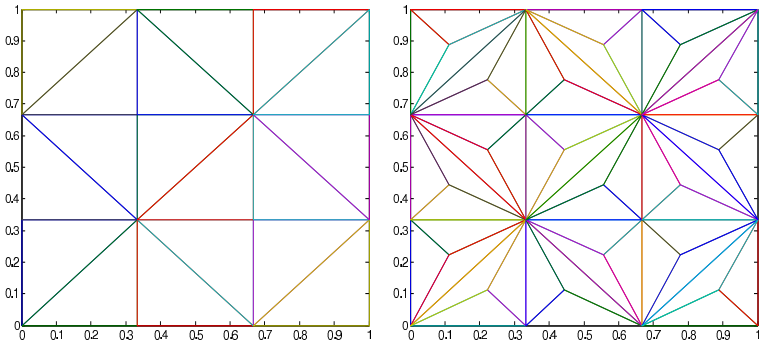

Figure 2: (LEFT) Regular 3×3 triangulation of the unit square; (RIGHT) The 3×3 barycenter refined triangulation of the unit square.

	$dim(X_h)$	$dim(Q_h^{TH})$	$\frac{dim(V_h)}{dim(X_h)}\%$	$\frac{dim(V_h^0)}{dim(X_h)}\%$
8×8	450	80	82.2	23.8
16×16	1922	288	85.0	27.6
20×20	3042	440	85.5	28.4
28×28	6050	840	86.1	29.2
32×32	7938	1088	86.3	29.5

Table 1: Dimensions of V_h and V_h^0 for regular triangulations of the unit square.

However, it is also possible that the limit solution could be very poor in the general case. For the mesh in Figure 3, counting degrees of freedom shows $dim(V_h^0) = 0$, which means that a divergence free velocity solution must be $\mathbf{0}$. This example shows that care must be taken in the mesh construction to avoid such an issue if γ is taken large.

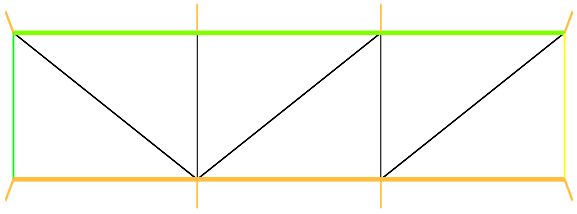

Figure 3: An mesh that yields $dim(V_h^0) = 0$

	$dim(X_h)$	$dim(Q_h^{TH})$	$\frac{dim(V_h)}{dim(X_h)}\%$	$\frac{dim(V_h^0)}{dim(X_h)}\%$
4×4	354	56	84.2	18.9
8×8	1474	208	85.9	21.9
12×12	3362	456	86.4	22.9
16×16	6018	800	86.7	23.5
20×20	9442	1240	86.9	23.8

Table 2: Dimensions of V_h and V_h^0 for barycenter refined triangulations of the unit square.

5 2D Numerical Experiments

In this section we investigate the convergence theory of the previous section. We numerically verify that on barycenter refined meshes with $k \geq d$, that as the grad-div parameter goes to infinity the TH approximations to NSE converge to the SV approximation. We also consider the general case, and the limiting behavior of the grad-div stabilized TH solutions there. Lastly, we discuss the choice of an optimal γ if mass conservation is explicitly accounted for in the objective function.

5.1 Numerical Experiment 1: 2d channel flow around a cylinder on a barycenter refined mesh

The benchmark problem of 2d channel flow around a cylinder has been studied in numerous works, e.g. [29, 13, 14, 16], and is well documented in [29]. The domain is the rectangle $[0,2.2]\times[0,0.41]$ representing the channel with flow in the positive x direction, with a circle radius 0.05 centered at $(0.2,0.2)$ representing the cylinder. No slip boundary conditions are prescribed on the top and bottom of the channel as well as on the cylinder, and the time dependent inflow and outflow velocity profiles are given by

$$\mathbf{u}(0,y,t) = \mathbf{u}(2.2,y,t) = \left[\frac{6}{0.41^2}\sin(\pi t/8)y(0.41-y),0\right]^T, \quad 0\leq y\leq 0.41.$$

The forcing function is set to zero, $\mathbf{f}=\mathbf{0}$, and the viscosity at $\nu = 0.001$, providing a time dependent Reynolds number, $0\leq Re(t)\leq 100$. The initial condition is $\mathbf{u}=\mathbf{0}$, and we compute to final time $T=8$ with time-step $\Delta t = 0.01$.

An accurate approximation of this flow's velocity field will show a vortex street forming behind the cylinder by $t=4$, and a fully formed vortex street by $t=7$. However, there is more than one way to measure accuracy. That is, even if the vortex street forms and the velocity vector field "appears" correct, if the velocity field does not conserve mass, then for many applications the solution may be unacceptable.

Solutions are computed for (P_2,P_1^{disc}) SV elements and for (P_2,P_1) TH elements with $\gamma = 0,\ 1,\ 100,\ 10{,}000$, all on the same barycenter refined mesh. This provides 6,578 velocity degrees of freedom, dof, and 4,797 pressure dof for the SV pressure, and 845

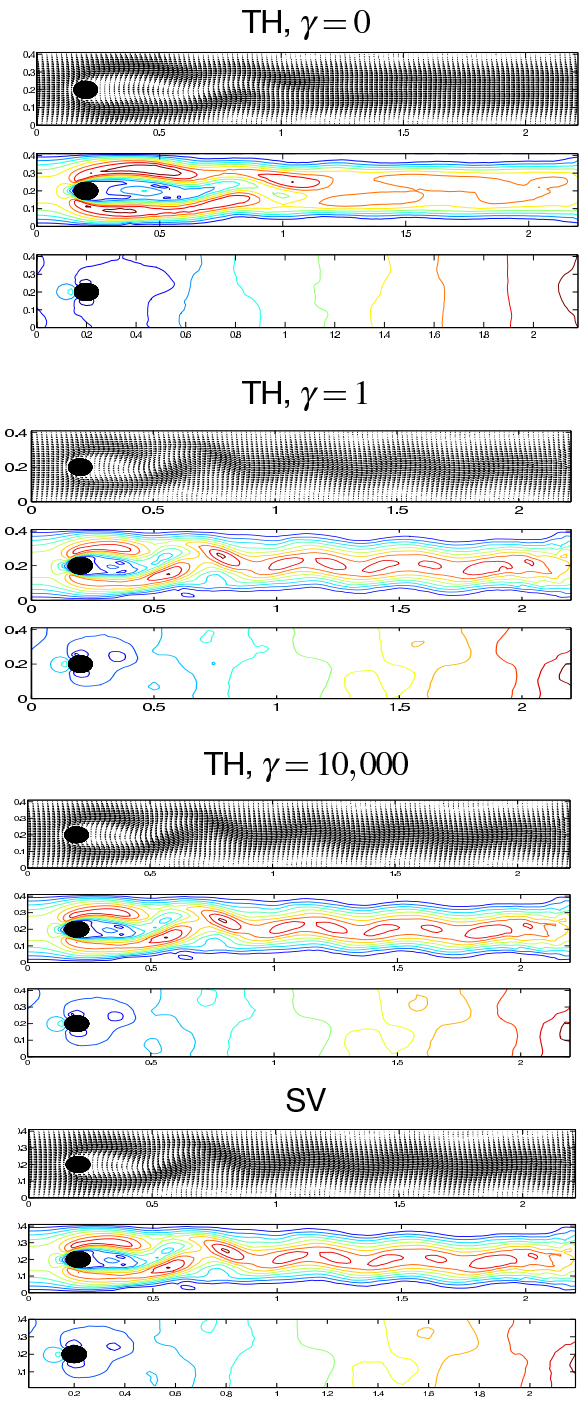

Figure 4: The t=7 velocity fields, speed contours, and pressure contour plots for approximations obtained using TH elements without grad-div stabilization (top), TH elements with $\gamma = 1$ (second from top), TH elements with $\gamma = 10,000$ (third from top), and the SV element approximation (bottom), on a barycentric mesh and $k = 2$. Convergence to the SV approximation as γ increases is clear. The SV and TH with $\gamma = 10,000$ approximations are nearly indistinguishable and agree well with known results [29, 13, 14]. Some slight differences with these and the plotted solution for TH elements with $\gamma = 1$ can be seen in the speed contours, and the $\gamma = 0$ solution is clearly underresolved.

pressure degrees of freedom for the TH simulation. Results of these simulations are shown in Table 3, and Figures 4 and 5.

γ	$\left\|\left\|\nabla \mathbf{u}_{TH}^{\gamma}(t=7) - \nabla \mathbf{u}_{SV}(t=7)\right\|\right\|$
0	5.7086
1	0.7616
100	7.9856e-3
10,000	8.5311e-5

Table 3: The table above shows convergence of the grad-div stabilized TH approximations to the SV approximation for Numerical Experiment 1.

Table 3 shows convergence of the TH approximations to the SV approximation as $\gamma \rightarrow \infty$. This agrees with the theory of Section 3. Figure 4 shows the plots of the velocity field, speed contours and pressure contours for SV and TH approximations with $\gamma = 0,\ 1,\ 100,\ 10{,}000$. The convergence as γ gets large of the TH approximations to the SV approximation is clear.

The benefit to mass conservation of increasing γ is shown in Figure 5. Here we see with $\gamma = 10{,}000$, excellent mass conservation is achieved. Also we note that for the unstabilized TH approximation, $\left\|\nabla \cdot \mathbf{u}_h^n\right\| = O(1)$.

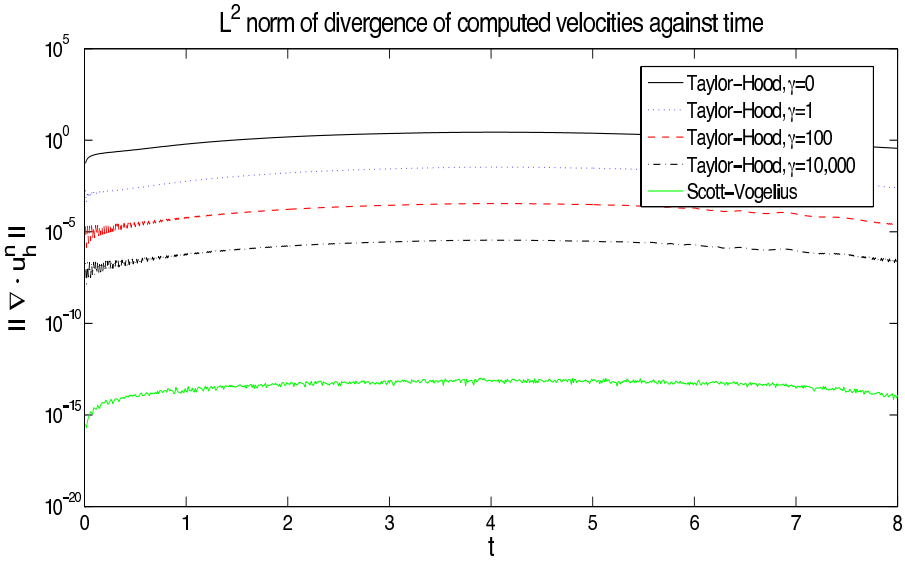

Figure 5: Shown above are the plots of $\left\|\nabla \cdot \mathbf{u}_h^n\right\|$ vs. time for the SV and TH approximations for Numerical Experiment 1, with varying γ.

5.2 Numerical Experiment 2: The 3d driven cavity

In 3d, SV elements require $k \geq 3$. Here we compare the (P_3, P_2^{disc}) SV approximation with that obtained using by grad-div stabilized (P_3, P_2) TH elements.

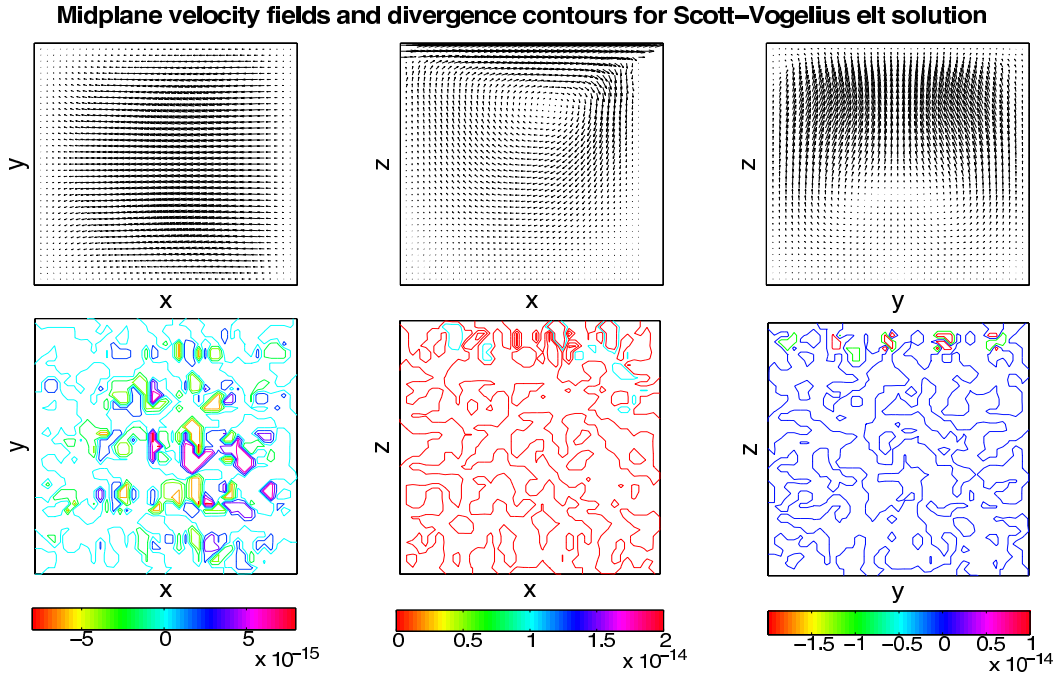

Figure 6: We see the expected velocity profiles for the lid-driven cavity problem with div $\mathbf{u}_h$ close to machine epsilon.

We next consider the benchmark problem of the 3d lid-driven cavity. This problem has been well-studied, [32, 23], and the description is as follows. The domain Ω is the $(-1,1)^3$ cube, for boundary conditions the top of the box (lid) is prescribed the velocity $\mathbf{u} = [1,0,0]^T$ with the velocity on the the sides and bottom set to zero ($\mathbf{u} = \mathbf{0}$), and the viscosity $\nu = 1/50$, giving the Reynolds' number $Re = 2 \cdot 1 \cdot 50 = 100$. We compute with a barycenter refinement of a uniform tetrahedral mesh (as discussed in Section 2), consisting of 51,119 total dof for the TH elements (46,038 velocity and 5,081 pressure) and 76,038 total dof for SV elements (46,038 velocity and 30,000 pressure). The problem is solved directly for the steady state approximation with a Newton iteration, using as the initial guess $\mathbf{u}(\mathbf{x}) = \mathbf{0},\ \mathbf{x} \in \Omega$. Five iterations were required to converge to a tolerance of 10^{-10} for each of the tests.

We compare the SV approximation and TH approximations with stabilization parameters $\gamma = 0,\ 1,\ 100,\ 10{,}000$. Plots of the TH ($\gamma = 0$) and SV approximations' midplane velocity vector fields and divergence contours are presented in Figures 6-7. A visual inspection of the velocity fields indicates they appear the same, and in agreement with the known solution [32]. However, the divergence contours show these solutions are

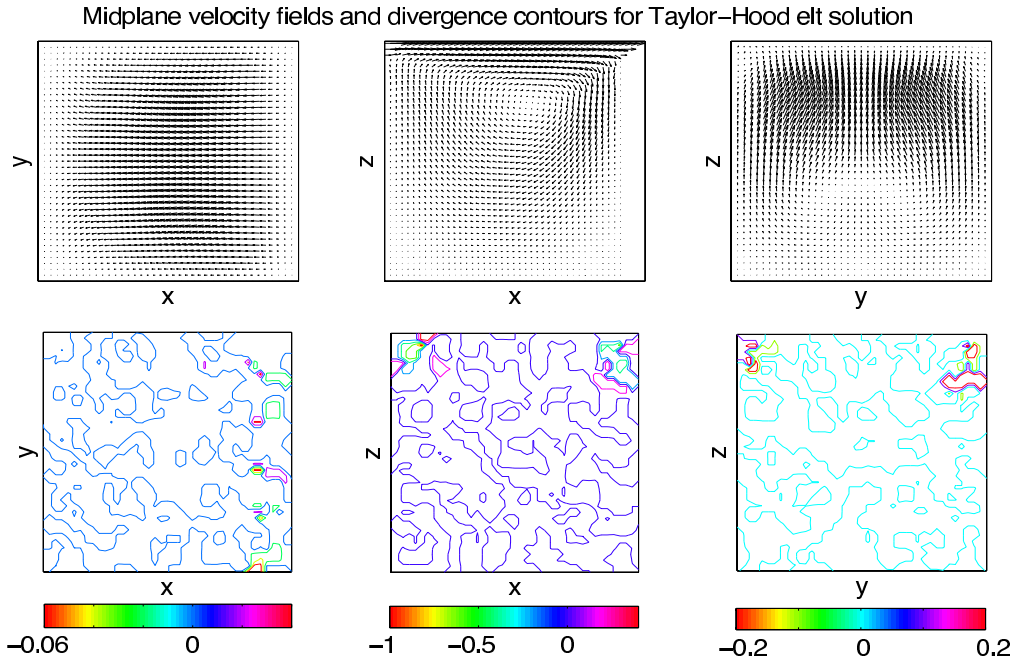

Figure 7: For TH with $\gamma = 0$, we see the expected velocity profiles for the lid-driven cavity problem, with non-negligible error for div $\mathbf{u}_h$.

in fact quite different. While the SV solution conserves mass up to roundoff error, the TH solution has O(1) mass conservation in the upper corners, and thus has poor physical accuracy. For the TH approximations using grad-div stabilization, we observe the velocity vector fields look identical to TH and SV plots as in Figures 6 and 7, and the magnitude of the divergence contours decreases as γ increases (pictures omitted).

The convergence of the TH velocity approximations to the SV velocity approximation can be seen in Table 4, giving verification to the theory of Section 3. Also shown in this table is the improvement in mass conservation from raising γ.

γ	$\|\|\nabla \mathbf{u}_{TH}^{\gamma} - \nabla \mathbf{u}_{SV}\|\|$	$\|\|\nabla \cdot \mathbf{u}_{TH}^{\gamma}\|\|$
0	1.0653	4.601E-1
1	0.2093	5.409E-2
100	0.0029	7.056E-4
10,000	2.951E-5	7.081E-6

Table 4: Convergence of the grad-div stabilized TH approximations toward the SV approximation as $\gamma \to \infty$ for the $Re = 100$ 3d driven cavity problem.

5.3 Numerical Experiment 3: 2d flow around a cylinder on general meshes

For our next experiment, we explore the effect of larger γ with TH elements ($k=2$) on a non barycenter refined mesh. In Section 4, we prove that velocity solutions converge as $\gamma \to \infty$. It has also been documented in [22] that TH solutions can numerically deteriorate for larger γ. Illustrated in Figure 8 are TH solutions corresponding to $\gamma = 0,\ 1,\ 100,\ 10{,}000$, using a mesh that provides 7,414 velocity degrees of freedom and 915 pressure degrees of freedom. This mesh is somewhat finer that in Experiment 1, and we see in the plot of the solution in Figure 8 that the $\gamma = 0$ solution now has a more resolved velocity field than the unstabilized solution of Experiment 1.

From Figure 8, we note that as γ increases, the solutions appear to converge, in agreement with the theory from chapter 4. However, we also see some deterioration in the speed contour plot. Conservation of mass improves in the same manner as in Experiment 1 on the barycenter refined mesh (plot omitted). Also, interestingly, we note that the pressure solution appears to improve with increasing γ.

5.4 Numerical Experiment 4: Another take on optimal γ

Recent work with grad-div stabilization suggests that the optimal γ for many problems is $O(1)$ [25, 24, 16, 17, 22]. While we do not contest this conjecture, we suggest $O(1)$ should instead be a starting point to finding an optimal γ. Experiment 1 showed a situation where $\gamma = \infty$ was best, and for Experiment 3, $\gamma = 0$ was best for velocity, and γ large ($>> O(1)$) appeared best for pressure. Thus large variation can exist in the value of an optimal γ. Moreover, what one considers an optimal γ can change depending on criteria. Specifically, if mass conservation is important (as it often is) and a computed solution's incompressibility (or lack thereof) is factored in, e.g. if the $H(\mathrm{div})$ norm is used instead of L^2, then an optimal value of γ can change significantly. Recall the $H(\mathrm{div})$ norm is defined by

$$\|\phi\|_{H(\mathrm{div})} := \sqrt{\|\phi\|^2 + \|\nabla \cdot \phi\|^2}.$$

The setup for this experiment is as follows: Using the selected NSE solution

$$u = \begin{pmatrix} 2x^2(x-1)^2y(2y-1)(y-1) \\ -2x(x-1)(2x-1)y^2(y-1)^2 \end{pmatrix}, \quad p = \sin(x),$$

on the unit square domain with $\nu = 0.0001$, $h = 1/16$ (non barycenter refined) mesh, solutions were computed using $k=2$ TH elements and varying values of the parameter γ. The computed solution was then compared to the true solution, and the L^2 and $H(\mathrm{div})$ norms of the error were calculated. Results are given in Table 5, and show that the optimal γ for minimizing the L^2 and H^1 velocity error is $O(1)$. However, for the $H(\mathrm{div})$ velocity and the L^2 pressure errors, the optimal γ is significantly larger. In fact, the $H(\mathrm{div})$ velocity error for the $\gamma = 100$ solution is less than half of that for $\gamma = O(1)$.

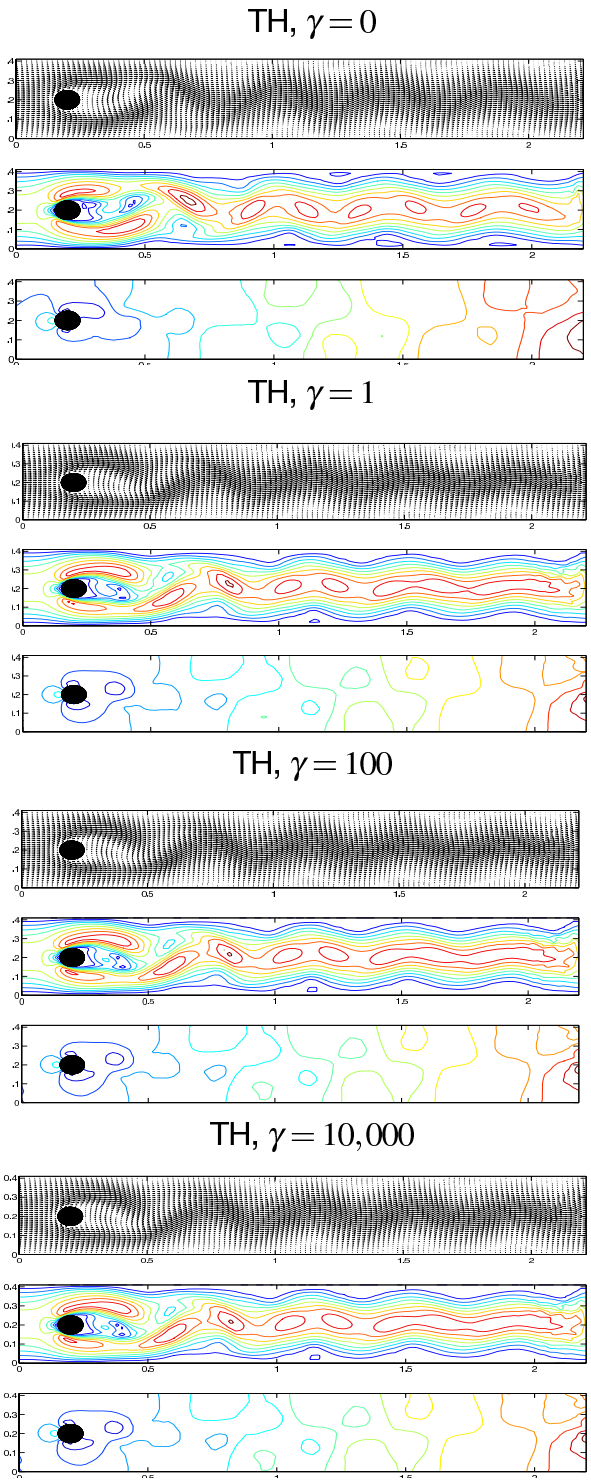

Figure 8: The t=7 velocity fields, speed contours, and pressure contour plots for solutions obtained using TH elements without grad-div stabilization (TOP), TH elements with $\gamma = 1$, $\gamma = 100$, and $\gamma = 10{,}000$ (BOTTOM), using a general (non-barycentric) mesh.

γ	$\|\mathbf{u}_{TH}^{\gamma} - \mathbf{u}_{true}\|$	$\|\mathbf{u}_{TH}^{\gamma} - \mathbf{u}_{true}\|_{H^1}$	$\|\mathbf{u}_{TH}^{\gamma} - \mathbf{u}_{true}\|_{H(\mathrm{div})}$	$\|p_{TH}^{\gamma} - p_{true}\|$
0	6.61E-2	3.28E-1	2.99E-1	8.5010E-5
0.1	5.53E-5	4.50E-3	4.77E-4	7.3178E-5
1	**2.67E-5**	**2.12E-3**	5.78E-5	7.3165E-5
10	2.72E-5	2.15E-3	2.77E-5	7.3165E-5
100	2.73E-5	2.16E-3	**2.73E-5**	7.3165E-5
1,000	2.73E-5	2.16E-3	**2.73E-5**	**7.3164E-5**
10,000	2.73E-5	2.16E-3	**2.73E-5**	**7.3164E-5**
100,000	2.73E-5	2.16E-3	**2.73E-5**	**7.3164E-5**

Table 5: L^2, H^1 and $H(\mathrm{div})$ velocity errors and L^2 pressure error for various stabilization parameters for Numerical Experiment 4.

6 Conclusions and Future Directions

We have proven, and illustrated numerically, that as the grad-div stabilizaion parameter, γ, goes to ∞ the TH approximations ($k \geq d$) on a barycenter refined mesh converge to the SV approximation. On a regular mesh we have proven that the TH approximations converge to a pointwise divergence-free solution as $\gamma \to \infty$.

Little effort is needed to incorporate grad-div stabilization into an existing finite element approximation of the NSE. Also, due to the similarity of Taylor-Hood elements and Scott-Vogelius elements, many existing codes using Taylor-Hood elements can be easily converted to use Scott-Vogelius elements (provided the mesh is as specified above). Hence we believe the two methods discussed in this paper may be of significant interest to engineers and fluid dynamicists interested in better mass conservation with reasonable development cost.

The "optimal" choice for γ is an interesting and open question. In [22, 6] Olshanskii et al. investigated optimal values for γ. In [22] they remarked " ... the search of an optimal γ as a trade-off between mass and energy balance in the FE system." From their investigations, they found that an optimal value of $\gamma \in [0.1, 1.0]$ was optimal for minimizing the L^2 and H^1 errors in the TH approximations. Note that for $\gamma = O(1)$ in the numerical examples presented in Section 5 the TH approximations gave $\|\mathrm{div}(\mathbf{u}_h)\| > O(h)$, which for many physical problems would be unacceptable. If so, a more appropriate physical criteria for determining an optimal value for γ may be the $H(\mathrm{div})$ norm or to determine γ which minimizes the H^1 error subject to $\|\mathrm{div}(\mathbf{u}_h)\| < tol$. We plan to investigate appropriate choices for γ in subsequent work.

References

[1] M. Benzi, M. Olshanskii, and Z. Wang. Modified augmented Lagrangian preconditioners for the incompressible Navier-Stokes equations. *International Journal for*

Numerical Methods in Fluids, to appear, 2010.

[2] F. Brezzi and M. Fortin. *Mixed and Hybrid Finite Element Methods*. Springer-Verlag, 1991.

[3] B. Cockburn, G. Kanschat, and D. Schötzau. A note on discontinuous Galerkin divergence-free solutions of the Navier-Stokes equations. *J. Sci. Comput.*, 31(1-2):61–73, 2007.

[4] H. Elman, D. Silvester, and A. Wathen. *Finite Elements and Fast Iterative Solvers with Applications in Incompressible Fluid Dynamics*. Numerical Mathematics and Scientific Computation. Oxford University Press, Oxford, 2005.

[5] S. Ganesan and V. John. Pressure separation — A technique for improving the velocity error in finite element discretisations of the Navier-Stokes equations. *Appl. Math. Comp.*, 165(2):275–290, 2005.

[6] T. Gelhard, G. Lube, M.A. Olshanskii, and J.-H. Starcke. Stabilized finite element schemes with LBB-stable elements for incompressible flows. *J. Comput. Appl. Math.*, 177:243–267, 2005.

[7] V. Girault and P.-A. Raviart. *Finite Element Methods for Navier-Stokes equations : Theory and Algorithms*. Springer-Verlag, 1986.

[8] P. Gresho and R. Sani. *Incompressible Flow and the Finite Element Method*, volume 2. Wiley, 1998.

[9] M. Gunzburger. *Finite Element Methods for Viscous Incompressible Flow: A Guide to Theory, Practice, and Algorithms*. Academic Press, Boston, 1989.

[10] J. Heywood and R. Rannacher. Finite element approximation of the nonstationary Navier-Stokes problem. I. Regularity of solutions and second-order error estimates for spatial discretization. *SIAM Journal on Numerical Analysis*, 19(2):275–311, 1982.

[11] J. Heywood and R. Rannacher. Finite element approximation of the nonstationary Navier-Stokes problem. Part IV: Error analysis for the second order time discretization. *SIAM J. Numer. Anal.*, 2:353–384, 1990.

[12] V. John. *Large Eddy Simulation of Turbulent Incompressible Flows. Analytical and Numerical Results for a Class of LES Models*, volume 34 of *Lecture Notes in Computational Science and Engineering*. Springer-Verlag Berlin, Heidelberg, New York, 2004.

[13] V. John. Reference values for drag and lift of a two dimensional time-dependent flow around a cylinder. *International Journal for Numerical Methods in Fluids*, 44:777–788, 2004.

[14] A. Labovsky, W. Layton, C. Manica, M. Neda, and L. Rebholz. The stabilized extrapolated trapezoidal finite element method for the Navier-Stokes equations. *Comput. Methods Appl. Mech. Engrg.*, 198:958–974, 2009.

[15] W. Layton. *An Introduction to the Numerical Analysis of Viscous Incompressible Flows*. SIAM, 2008.

[16] W. Layton, C. Manica, M. Neda, M.A. Olshanskii, and L. Rebholz. On the accuracy of the rotation form in simulations of the Navier-Stokes equations. *J. Comput. Phys.*, 228(5):3433–3447, 2009.

[17] W. Layton, C. Manica, M. Neda, and L. Rebholz. Numerical analysis and computational comparisons of the NS-omega and NS-alpha regularizations. *Comput. Methods Appl. Mech. Engrg.*, to appear, 2009.

[18] A. Linke. *Divergence-free mixed finite elements for the incompressible Navier-Stokes Equation*. PhD thesis, University of Erlangen, 2007.

[19] A. Linke. Collision in a cross-shaped domain — A steady 2d Navier-Stokes example demonstrating the importance of mass conservation in CFD. *Comp. Meth. Appl. Mech. Eng.*, 198(41–44):3278–3286, 2009.

[20] G. Matthies and L. Tobiska. Mass conservation of finite element methods for coupled flow-transport problems. In G. Lube and G. Rapin, editors, *Proceedings of the International Conference on Boundary and Interior Layers*. BAIL, 2006.

[21] I.M. Navon. Implementation of a posteriori methods for enforcing conservation of potential enstrophy and mass in discretized shallow water equation models. *Monthly Weather Review*, 109:946–958, 1981.

[22] M. Olshanskii, G. Lube, T. Heister, and J. Löwe. Grad-div stabilization and subgrid pressure models for the incompressible Navier-Stokes equations. *Comp. Meth. Appl. Mech. Eng.*, 198:3975–3988, 2009.

[23] M. Olshanskii and L. Rebholz. Velocity-Vorticity-Helicity formulation and a solver for the Navier-Stokes equations. *Journal of Computational Physics*, to appear, 2010.

[24] M.A. Olshanskii. A low order Galerkin finite element method for the Navier-Stokes equations of steady incompressible flow: A stabilization issue and iterative methods. *Comp. Meth. Appl. Mech. Eng.*, 191:5515–5536, 2002.

[25] M.A. Olshanskii and A. Reusken. Navier-Stokes equations in rotation form: a robust multigrid solver for the velocity problem. *SIAM J. Sci. Comput.*, 23:1682–1706, 2002.

[26] M.A. Olshanskii and A. Reusken. Grad-Div stabilization for the Stokes equations. *Math. Comp.*, 73:1699–1718, 2004.

[27] B. Riviere. *Discontinuous Galerkin Methods for Solving Elliptic and Parabolic Equations: Theory and Implementation*. SIAM, 2008.

[28] H.-G. Roos, M. Stynes, and L. Tobiska. *Robust Numerical Methods for Singularly Perturbed Differential Equations*, volume 24 of *Springer Series in Computational Mathematics*. Springer, Berlin, 2nd edition, 2008.

[29] M. Schäfer and S. Turek. The benchmark problem 'flow around a cylinder' flow simulation with high performance computers II. *in E.H. Hirschel (Ed.), Notes on Numerical Fluid Mechanics*, 52, Braunschweig, Vieweg:547–566, 1996.

[30] H. Sohr. *The Navier-Stokes Equations, An Elementary Functional Analytic Approach*. Birhäuser Advanced Texts. Birkhäuser Verlag Basel, Boston, Berlin, 2001.

[31] R. Temam. *Navier-Stokes Equations : Theory and Numerical Analysis*. Elsevier North-Holland, 1979.

[32] K.L. Wong and A.J. Baker. A 3d incompressible Navier-Stokes velocity-vorticity weak form finite element algorithm. *International Journal for Numerical Methods in Fluids*, 38:99–123, 2002.

[33] S. Zhang. A new family of stable mixed finite elements for the 3d Stokes equations. *Math. Comp.*, 74(250):543–554, 2005.

[34] S. Zhang. A family of $Q_{k+1,k} \times Q_{k,k+1}$ divergence-free finite elements on rectangular grids. *SIAM J. Numer. Anal.*, 47(3):2090–2107, 2009.